

Determination of Absolute Configuration Using Concerted ab Initio DFT Calculations of Electronic Circular Dichroism and Optical Rotation: Bicyclo[3.3.1]nonane Diones

P. J. Stephens,^{*,†} D. M. McCann,[†] E. Butkus,[‡] S. Stončius,[‡] J. R. Cheeseman,[§] and M. J. Frisch[§]

Department of Chemistry, University of Southern California, Los Angeles, California 90089-0482, Department of Organic Chemistry, Vilnius University, Naugarduko 24, 2006 Vilnius, Lithuania, and Gaussian Inc., 340 Quinnipiac St., Building No. 40, Wallingford, Connecticut 06492-4050

pstephen@usc.edu

Received November 20, 2003

The *concerted* use of ab initio time-dependent density functional theory (TDDFT) calculations of transparent spectral region optical rotation and of circular dichroism has recently become practicable, permitting the *concerted* use of transparent spectral region optical rotation and circular dichroism in determining the absolute configurations of chiral molecules. Here, we report *concerted* TDDFT calculations of the transparent spectral region specific rotations and of the circular dichroism spectra originating in $n \rightarrow \pi^*$ C=O group excitations of four bicyclo[3.3.1]nonane diones, **1–4**. Comparison to experiment yields absolute configurations for **1–4**. For each dione, specific rotations and circular dichroism spectra give identical absolute configurations. Our results are consistent with previous work, with the exception of the Octant Rule-derived absolute configuration of the 2,9-dione.

Introduction

Chiral molecules exhibit electronic optical activity, i.e., electronic circular dichroism (CD) and optical rotation (OR). Mirror-image enantiomers of a chiral molecule exhibit mirror-image CD and OR. That is, at any wavelength, the CD and OR of the two enantiomers are equal in magnitude and opposite in sign. It follows that, in principle, the absolute configuration (AC) of a chiral molecule can be deduced from its CD and/or OR. In practice, the determination of AC requires a methodology for predicting the CD and/or OR of a molecule of known structure. A variety of methodologies have been devised for this purpose, ranging from empirical rules to ab initio quantum mechanical methods, and applied to the determination of AC.¹ However, until very recently, the methods developed have suffered from major limitations: in particular, they have generally been specific to the prediction of either CD or OR, but not both simultaneously, and they have generally been of limited applicability.

Very recently, a major advance has taken place in the prediction of CD and OR as a result of the exploitation of the ab initio quantum mechanical methodology of time-dependent density functional theory (TDDFT). It is now practicable to predict *simultaneously* both the CD and the transparent spectral region OR of a chiral molecule using TDDFT.² A number of studies using this new

methodology have documented the reliability of predicted CD or transparent spectral region OR for a variety of organic molecules.^{2,3} In a few cases, ACs have been determined via such calculations.⁴ However, to date CD or OR has been studied without simultaneous consideration of the complementary phenomenon. In this work, we report studies of the ACs of a set of chiral molecules in which their CD and transparent spectral region OR are analyzed using TDDFT calculations in a concerted

(2) (a) Stephens, P. J.; Devlin, F. J.; Cheeseman, J. R.; Frisch, M. J. *J. Phys. Chem. A* **2001**, *105*, 5356. (b) Mennucci, B.; Tomasi, J.; Cammi, R.; Cheeseman, J. R.; Frisch, M. J.; Devlin, F. J.; Gabriel, S.; Stephens, P. J. *J. Phys. Chem. A* **2002**, *106*, 6102. (c) Grimme, S. *Chem. Phys. Lett.* **2001**, *339*, 380. (d) Grimme, S.; Furche, F.; Ahlrichs, R. *Chem. Phys. Lett.* **2002**, *361*, 321. (e) Autschbach, J.; Patchkovskii, S.; Ziegler, T.; van Gisbergen, S. J. A.; Baerends, E. J. *J. Chem. Phys.* **2002**, *117*, 581. (f) Ruud, K.; Helgaker, T. *Chem. Phys. Lett.* **2002**, *352*, 533. (g) Furche, F.; Ahlrichs, R.; Wachsmann, C.; Weber, E.; Sobanski, A.; Vogtle, F.; Grimme, S. *J. Am. Chem. Soc.* **2000**, *122*, 1717. (h) Autschbach, J.; Ziegler, T.; van Gisbergen, S. J. A.; Baerends, E. J. *J. Chem. Phys.* **2002**, *116*, 6930.

(3) (a) Stephens, P. J.; Devlin, F. J.; Cheeseman, J. R.; Frisch, M. J.; Mennucci, B.; Tomasi, J. *Tetrahedron: Asymmetry* **2000**, *11*, 2443. (b) Stephens, P. J.; Devlin, F. J.; Cheeseman, J. R.; Frisch, M. J. *Chirality* **2002**, *14*, 288. (c) Grimme, S.; Bahlmann, A.; Haufe, G. *Chirality* **2002**, *14*, 793. (d) Polavarapu, P. L. *Chirality* **2002**, *14*, 768. (e) Polavarapu, P. L.; Petrovic, A.; Wang, F. *Chirality* **2003**, *15*, S143. (f) Wiberg, K. H.; Vaccaro, P. H.; Cheeseman, J. R. *J. Am. Chem. Soc.* **2003**, *125*, 1888. (g) Diedrich, C.; Grimme, S. *J. Phys. Chem. A* **2003**, *107*, 2524.

(4) (a) Stephens, P. J.; Devlin, F. J.; Cheeseman, J. R.; Frisch, M. J.; Rosini, C. *Org. Lett.* **2002**, *4*, 4595. (b) Stephens, P. J.; Devlin, F. J.; Cheeseman, J. R.; Frisch, M. J.; Bortolini, O.; Besse, P. *Chirality* **2003**, *15*, S57. (c) Wang, F.; Wang, Y.; Polavarapu, P. L.; Li, T.; Drabowicz, J.; Pietrusiewicz, K. M.; Zygo, K. *J. Org. Chem.* **2002**, *67*, 6539. (d) Polavarapu, P. L. *Angew. Chem., Int. Ed.* **2002**, *41*, 4544. (e) Furche, F.; Ahlrichs, R. *J. Am. Chem. Soc.* **2002**, *124*, 3804. (f) Wang, Y.; Raabe, G.; Repges, C.; Fleischhauer, J. *Int. J. Quantum Chem.* **2003**, *93*, 265.

[†] University of Southern California.

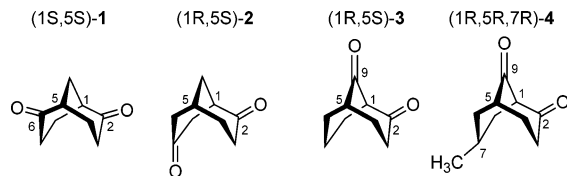
[‡] Vilnius University.

[§] Gaussian Inc.

(1) Eliel, E. L.; Wilen, S. H. *Stereochemistry of Organic Compounds*; Wiley: New York, 1994; Chapter 13.

manner. The use of *both* CD *and* transparent spectral region OR substantially enhances the reliability of the AC deduced.

For this study, we have chosen a set of four bicyclo[3.3.1]nonane diones, **1–4**. Compounds **1–4** are chiral



structures by virtue of carbonyl substitution on the bicyclo[3.3.1]nonane skeleton. Their exploitation in stereo- and enantioselective synthesis was recently discussed.⁵ In addition, carbonyl derivatives of the bicyclo[3.3.1]nonane framework are quite commonly found in nature as constituents of natural products or their metabolites.⁶ CD has played a major role in the elucidation of the ACs of molecules **1–3**.^{7–11} On the other hand, OR has not been previously employed in deducing the ACs of **1–4**.

The 2,6-dione (**1**) has been the most extensively studied in optically active form. A variety of methods have been used to obtain enantiomers of **1**, including desulfurization of 2-thia-adamantane-4,8-dione,⁷ oxidation of the corresponding 2,6-diol,⁸ Baker's yeast resolution of racemic **1**,^{11–14} alcohol dehydrogenase resolution of racemic **1**,^{15,16} and chiral column chromatography of racemic **1**.⁹ Transparent spectral region specific rotations have been reported by several authors.^{8,9,11,12,14–16} UV CD data have also been reported by several authors.^{7–9} The AC of **1** has been inferred by using the UV CD,^{7–9} together with the Octant Rule,¹⁷ and confirmed (1) via synthesis from/of the stereochemically characterized 3-COOH-cyclohexanone⁸ and (2) by using the UV CD, together with calculations using a methodology of Tinoco and Schellman.¹⁰ All methods used to date have consistently given the AC (1*S*,5*S*)-(+)/(1*R*,5*R*)-(-).

Optically active 2,7-dione, **2**, has been obtained by chiral chromatography of racemic **2** and by synthesis from optically active **1**.¹¹ The UV CD and transparent spectral region specific rotation have been reported.¹¹ The AC of **2** was inferred both (1) from the UV CD, using the

Octant Rule, and (2) via synthesis from **1**, using the known AC of **1**. The AC arrived at was (1*R*,5*S*)-(+)/(1*S*,5*R*)-(-).

Optically active 2,9-dione, **3**, has been obtained by using chiral chromatography of racemic **3**⁹ and via asymmetric cyclization of an enamine of 2-(methoxymethyl)pyrrolidine.^{18,19} Transparent spectral region specific rotations^{9,18} and UV CD⁹ have been reported. The AC of **3** was first determined by using the UV CD and the Octant Rule, with the result (1*R*,5*S*)-(+)/(1*S*,5*R*)-(-).⁹ Subsequently, calculations of the UV CD using a Tinoco–Schellman methodology led to the opposite conclusion: (1*S*,5*R*)-(+)/(1*R*,5*S*)-(-).¹⁰ The latter AC was supported by a mechanistic analysis of the synthesis via asymmetric cyclization.¹⁸

Optically active *exo*-7-methyl-2,9-dione, **4**, has been obtained via asymmetric cyclization of an enamine of 2-(methoxymethyl)pyrrolidine.¹⁸ Transparent spectral region specific rotations, but not UV CD, were reported. The AC (1*S*,5*S*,7*S*)-(+)/(1*R*,5*R*,7*R*)-(-) of **4** was inferred via mechanistic analysis of the synthesis.¹⁸

In this work, we report new CD and OR data for samples of **1–4** of higher enantiomeric excess (ee) than used before, together with TDDFT calculations of the CD and OR of **1–4**. Our principal goal is to evaluate the efficacy of TDDFT CD and OR calculations in determining the ACs of **1–4**. These molecules are conformationally flexible and their experimental CD and OR are for equilibrium mixtures of conformers. Conformational analyses are therefore a prerequisite for CD and OR calculations.

Methods

NMR. ¹H NMR spectra were recorded on a 400-MHz spectrometer in deuterated chloroform.

Chromatography. Enantiomeric excesses were determined using a gas chromatograph equipped with a split/splitless injector and flame ionization detector together with a beta-Dex 120 fused silica capillary column of 0.25 μm film thickness, 30 × 0.25 mm i.d.

Synthetic Methods. (+)-**1**: (+)-**1** was synthesized via enzymatic resolution of (±)-**1** using Baker's yeast, following the procedure described previously.^{11,13,14} The ee of the resulting (+)-**1** was >99%.

(+)-**2**: (+)-**2** was synthesized from (+)-**1** following the procedure described previously.¹¹ The ee of the resulting (+)-**2** was 100%.

(+)-**3**: (+)-**3** was obtained via asymmetric synthesis starting from (2*R*)-1-(cyclohexen-1-yl)-2-(methoxymethyl)pyrrolidine following the procedure described previously.¹⁸ The ee of the resulting (+)-**3** was 80%. ¹H NMR: δ 3.15 (1H, m, H-1), 2.81 (1H, m), 2.63 (1H, m), 2.48 (1H, m), 2.38–1.92 (8H, m).

(-)-**4**: (-)-**4** was obtained via asymmetric synthesis starting from (2*S*)-1-(4-methylcyclohexen-1-yl)-2-(methoxymethyl)pyrrolidine following the procedure described previously.¹⁸ The ee of the resulting (-)-**4** was 83%. ¹H NMR: δ 3.09 (1H, m, H-1), 2.76 (1H, m, H-5), 2.68 (1H, two q, *J* = 6 Hz), 2.45 (1H, m, H-3_{exo}), 2.34 (1H, m, H-3_{endo}), 2.20–1.75 (6H, m), 0.93 (3H, d, *J* = 6 Hz).

Calculations. Conformers of diones **1–4** were built using Cerius² 20 and optimized using the CFF95 molecular mechanics force field therein.²¹ CFF95 structures were further optimized

(5) Butkus, E. *Synlett* **2001**, 1827.
 (6) For some recent examples see: Fraga, B. M. *Nat. Prod. Rep.* **2002**, *19*, 650. Usuda, H.; Kanai, M.; Shibasaki, M. *Tetrahedron Lett.* **2002**, *43*, 3621. Sepssard, S. J.; Stoltz, B. M. *Org. Lett.* **2002**, *4*, 1943.
 (7) Snatzke G., Wolfram, B. *Tetrahedron* **1972**, *28*, 655.
 (8) Gerlach, H. *Helv. Chim. Acta* **1978**, *61*, 2773.
 (9) Berg, U.; Butkus, E. *J. Chem. Res., Synop.* **1993**, 116.
 (10) Berg, U.; Butkus, E. *J. Chem. Res., Synop.* **1994**, 356.
 (11) Butkus, E.; Stoncius, S.; Zilinskas, A. *Chirality* **2001**, *13*, 694.
 (12) Hoffmann G.; Wiartalla, R. *Tetrahedron Lett.* **1982**, *23*, 3887.
 (13) Butkus, E.; Berg, U.; Zilinskas, A.; Kubilius, R.; Stoncius, S. *Tetrahedron: Asymmetry* **2000**, *11*, 3053.
 (14) Butkus, E.; Zilinskas, A.; Stoncius, S.; Rozenbergas, R.; Urbanová, M.; Setnicka, N.; Bour, P.; Volka, K. *Tetrahedron: Asymmetry* **2002**, *13*, 633.
 (15) Malinauskiene, J.; Kadziauskas, P.; Malinauskas, A.; Kulyš, J. *Monatsh. Chem.* **1999**, *130*, 1513.
 (16) Butkus, E.; Berg, U.; Malinauskiene, J.; Sandström, J. *J. Org. Chem.* **2000**, *65*, 1353.
 (17) (a) Lightner, D. A.; Gurst, J. E. *Organic Conformational Analysis and Stereochemistry*; Wiley: New York, 2000; Chapter 4, pp 63–94. (b) Lightner, D. A. In *Circular Dichroism: Principles and Applications*; Berova, N.; Nakanishi, K., Woody, R. W., Eds.; Wiley: New York, 2000; Chapter 10, pp 261–303.

(18) Butkus E.; Stoncius, A. *Synlett* **1999**, 234.
 (19) Butkus, E.; Malinauskiene, J.; Stoncius, S. *Org. Biomol. Chem.* **2003**, *1*, 391.
 (20) Cerius² 3.0; Molecular Simulations Inc.: San Diego, CA.

using the MMFF94 molecular mechanics method²² and the AM1 and PM3 semiempirical methods²³ with SPARTAN 02.²⁴ In addition, CFF95 structures were further optimized using the Hartree–Fock (HF)/6-31G** and density functional theory (DFT)/B3LYP/6-31G* ab initio methods using GAUSSIAN 98.²⁵ The completeness of the conformational analysis was confirmed using the Monte Carlo conformational searching routine of SPARTAN 02 with the MMFF94, AM1, and PM3 methods. For the B3LYP/6-31G* structures relative free energies were also calculated with GAUSSIAN 98.

Optical rotations and electronic excitation energies, oscillator strengths, and rotational strengths were calculated for all conformers of **1–4** using GAUSSIAN 03.²⁵ B3LYP/6-31G* geometries were used. Optical rotations were calculated using time-dependent DFT (TDDFT)^{2a,2b} and gauge-invariant atomic orbitals (GIAOs).²⁶ The functional was B3LYP and the basis set was aug-cc-pVDZ, a combination shown to provide excellent reliability in the prediction of optical rotations.^{2a} Electronic excitations were calculated using TDDFT, without using GIAOs.²⁷ The functional and basis set were again B3LYP and aug-cc-pVDZ for consistency with the optical rotation calculations. Optical rotations calculated using the TDDFT/GIAO methodology are origin-independent. Rotational strengths calculated using TDDFT without GIAOs are origin-independent when obtained via the velocity representation, but not when obtained via the length representation. In this work both are calculated. For length rotational strengths the origin is the center of positive charge. Optical rotations and rotational strengths were conformationally averaged using B3LYP/6-31G* conformational free energy differences, together with Boltzmann statistics.

Results

Bicyclo[3.3.1]nonane-2,6-dione (1). (a) **Conformational analysis:** MM2 calculations by Berg and Butkus¹⁰ found two conformations of **1**, chair-chair (CC) and chair-boat (CB), the latter being 0.37 kcal/mol higher in energy. A subsequent study by Alkauskas et al.²⁸ at the HF/6-31G and HF/6-31G** levels found four stable conformations, CC, CB, and two higher energy boat-boat (BB) conformations. The relative enthalpies reported are given in Table 1. We have extended these previous studies to include the CFF95 and MMFF94 molecular mechanics methods, the AM1 and PM3 semiempirical methods, and the B3LYP/6-31G* ab initio method, with the results summarized in Table 1. All methods predict

that the CC conformation is lowest in energy, and that the CB conformation is the next highest. The energy difference varies considerably with method, ranging from 0.16 (AM1) to 1.77 kcal/mol (PM3). Using B3LYP/6-31G*, the most reliable of the methods used here, the energy difference is 0.94 kcal/mol. Predictions for the BB conformations vary more widely with method. The MMFF94, AM1, and PM3 methods predict only one stable BB conformation. CFF95, HF/6-31G**, and B3LYP/6-31G* methods predict two BB conformations with energy differences of ~0.5, ~1.1, and ~2.0 kcal/mol, respectively. With the exception of the AM1 BB conformation, all BB conformations are >3 kcal/mol higher than the CC conformation. At the B3LYP/6-31G* level, relative free energies (ΔG) have been calculated in addition to relative energies (ΔE), with the results given in Table 1. ΔG for the CB conformation is considerably smaller (0.58 kcal/mol) than ΔE (0.94 kcal/mol). Percentage populations have been calculated based on ΔE and ΔG values, using Boltzmann statistics and $T = 298$ K, with the results given in Table 1. At room temperature we predict that both CC and CB conformers are significantly populated, CC being predominant, and that together they constitute >99% of the equilibrium mixture of CC, CB, and BB conformers, a conclusion consistent with the earlier work of Berg and Butkus.¹⁰

(b) **Electronic CD:** Snatzke and Wolfram⁷ and Gerlach⁸ reported positive CD near 300 nm for (+)-**1**, attributable to the $n \rightarrow \pi^*$ transitions of the C=O groups of **1**. By using the Octant Rule and assuming the conformation of **1** to be CC, the AC (1*S*,5*S*)-(+)-**1** was deduced. Berg and Butkus⁹ reported the experimental CD of (-)-**1**. The CD at 297 nm was negative for (-)-**1**, consistent with the earlier reports, as was the AC (1*R*,5*R*)-(-)-**1**, deduced using the Octant Rule. Subsequently, Berg and Butkus¹⁰ reported calculations of the CD of **1**, using a methodology of Tinoco and Schellman, assuming an equilibrium mixture of CC and CB conformations (75% and 25%, respectively). The CC and CB conformations of (1*R*,5*R*)-**1** were predicted to exhibit strong negative and weak positive $n \rightarrow \pi^*$ CD respectively, resulting in net negative CD, consistent with the Octant Rule-based AC.

In this work we have remeasured the ECD of **1**, using a sample of (+)-**1** of much higher ee (>99%) than used in the earlier work (55–60%). This spectrum is shown in Figure 1. Integration of the ECD spectrum (over the range 240–335 nm) yields an experimental value for the net rotational strength of the $n \rightarrow \pi^*$ transitions of $+7.0 \times 10^{-40}$ esu² cm².

Excitation energies, oscillator strengths, and rotational strengths have been predicted for the conformations of (1*S*,5*S*)-**1**, at their B3LYP/6-31G* equilibrium geometries, using B3LYP and the aug-cc-pVDZ basis set, with the results given in Table 1. For each conformer two low-energy transitions are predicted within the range 295–315 nm, attributable to $n \rightarrow \pi^*$ excitations of the C=O groups, well-separated from the next-highest excitations. The CD spectrum of the equilibrium mixture of conformers is plotted in Figure 1. Due to the >99% population of the CC and CB conformers, only these two conformers contribute significantly. For the dominant CC conformation of (1*S*,5*S*)-**1**, the two $n \rightarrow \pi^*$ excitations at 302 and 300 nm are predicted to have strong positive and weak negative CD, respectively. For the higher energy CB

(21) For earlier versions of the CFF force field see: (a) Dinur, U.; Hagler, A. T. *Rev. Comput. Chem.* **1991**, *4*, 1991. (b) Maple, J. R.; Dinur, U.; Hagler, A. T. *Proc. Natl. Acad. Sci. U.S.A.* **1988**, *85*, 5350.

(22) Halgren, T. A. *J. Comput. Chem.* **1996**, *17*, 490.

(23) AM1: Dewar, M. J. S.; Zoebisch, E. G.; Healey, E. F.; Stewart, J. J. P. *J. Am. Chem. Soc.* **1985**, *107*, 3902. PM3: Stewart, J. J. P. *J. Comput. Chem.* **1989**, *10*, 209.

(24) *Spartan 02*; Wavefunction Inc.: Irvine, CA.

(25) Frisch, M. J.; Trucks, G. W.; Schlegel, H. B.; Scuseria, G. E.; Robb, M. A.; Cheeseman, J. R.; Zakrzewski, V. G.; Montgomery, J. A., Jr.; Stratmann, R. E.; Burant, J. C.; Dapprich, S.; Millam, J. M.; Daniels, A. D.; Kudin, K. N.; Strain, M. C.; Farkas, O.; Tomasi, J.; Barone, V.; Cossi, M.; Cammi, R.; Mennucci, B.; Pomelli, C.; Adamo, C.; Clifford, S.; Ochterski, J.; Petersson, G. A.; Ayala, P. Y.; Cui, Q.; Morokuma, K.; Malick, D. K.; Rabuck, A. D.; Raghavachari, K.; Foresman, J. B.; Cioslowski, J.; Ortiz, J. V.; Stefanov, B. B.; Liu, G.; Liashenko, A.; Piskorz, P.; Komaromi, I.; Gomperts, R.; Martin, R. L.; Fox, D. J.; Keith, T.; Al-Laham, M. A.; Peng, C. Y.; Nanayakkara, A.; Gonzalez, C.; Challacombe, M.; Gill, P. M. W.; Johnson, B. G.; Chen, W.; Wong, M. W.; Andres, J. L.; Head-Gordon, M.; Replogle, E. S.; Pople, J. A. *Gaussian 98 and 03*; Gaussian, Inc.: Pittsburgh, PA.

(26) Cheeseman, J. R.; Frisch, M. J.; Devlin, F. J.; Stephens, P. J. *J. Phys. Chem. A* **2000**, *104*, 1039.

(27) Following the methodology of refs 2g and 2h.

(28) Alkauskas, A.; Ceponius, J.; Mikulskiene, B.; Aleksa, V.; Butkus, E.; Sablinskas, V. *J. Mol. Struct.* **2001**, *563*, 517.

TABLE 1. 2,6-Dione, 1: Conformational Energies, Specific Rotations, and Circular Dichroism

Conformations ^a											
	MM2 ^b ΔE	CFF95 ΔE	MMFF94 ΔE	AM1 ΔE	PM3 ΔE						
CC	0	0	0	0	0						
CB	0.37	1.68	0.43	0.16	1.77						
BBa		5.97									
BB			3.50	1.70	4.32						
BBb		6.49									
HF/6-31G ^c											
	ΔH	HF/6-31G** ΔE		B3LYP/6-31G* ΔE		B3LYP/6-31G* ΔG		B3LYP/6-31G* $P(\Delta E)^d$		B3LYP/6-31G* $P(\Delta G)^d$	
CC	0	0	0	0	0	82.7	72.4				
CB	0.79	0.83	0.81	0.94	0.58	16.8	27.2				
BBa	3.73	3.91	3.82	3.12	3.15	0.4	0.4				
BB											
BBb	5.04	5.06	4.92	5.11	4.72	0.0	0.0				
Specific Rotation											
calcd ^e [α]											
λ (nm)	CC	CB	BBa	BBb	av (ΔE) ^f	av (ΔG) ^f	exptl ^g [α]				
D	334	70	-175	-82	287	260	211/188/213				
578							226/178/222				
546	411	91	-203	-97	354	322	263/206/260				
436							538/410/530				
365	1945	704	-121	-189	1727	1600	1184/860/1171				
Circular Dichroism											
calcd ^e for CC					calcd ^e for CB					exptl ^h	
E (eV)	λ (nm)	f^j	R_{vel}^i	R_{length}^i	E (eV)	λ (nm)	f^j	R_{vel}^i	R_{length}^i	λ (nm)	R^i
4.112	302	0.0005	14.56	15.28	4.115	301	0.0001	1.45	1.37	297	7.0
4.133	300	0.0000	-0.28	-0.22	4.179	297	0.0003	9.14	9.69		
5.155	241	0.0003	-0.78	-0.78	4.963	250	0.0024	-3.55	-3.63		
5.173	240	0.0038	-2.73	-2.85	5.358	231	0.0079	-8.23	-8.55		
calcd ^e for BBa					calcd ^e for BBb						
E (eV)	λ (nm)	f^j	R_{vel}^i	R_{length}^i	E (eV)	λ (nm)	f^j	R_{vel}^i	R_{length}^i		
3.934	315	0.0003	7.60	6.95	4.154	298	0.0001	7.82	7.62		
4.076	304	0.0000	-3.18	-2.19	4.190	296	0.0001	-4.16	-4.23		
5.212	238	0.0005	-10.42	-11.33	5.252	236	0.0001	-1.84	-1.93		
5.336	232	0.0037	-8.86	-8.77	5.275	235	0.0024	-13.79	-14.39		

^a Relative energies in kcal/mol. For HF/6-31G and HF/6-31G** relative enthalpies in kcal/mol are also given. For B3LYP/6-31G* relative free energies in kcal/mol are also given. ^b Reference 10. ^c Reference 28. ^d Percentage populations obtained from ΔE and ΔG values, using Boltzmann statistics and $T = 298$ K. ^e B3LYP/aug-cc-pVDZ at the B3LYP/6-31G* geometry of each conformation. AC is 1*S*,5*S*. ^f $\text{av}(\Delta E)$ and $\text{av}(\Delta G)$ [α] values are conformational averages based on B3LYP/6-31G* ΔE and ΔG values, respectively. ^g For (+)-**1**: solvents are dioxane (c 0.135)/MeOH (c 0.28)/acetone (c 0.25); ee is >99% (chiral chromatography); temperature is 22 °C. ^h For (+)-**1**: solvent is 95% EtOH; ee is >99% (chiral chromatography). ⁱ R values in 10^{-40} esu² cm². ^j Oscillator strengths.

conformation, the two $n \rightarrow \pi^*$ excitations at 301 and 297 nm are predicted to have weak and strong positive CD, respectively. We predict a net rotational strength for the $n \rightarrow \pi^*$ transitions of (1*S*,5*S*)-**1** of $+13.2 \times 10^{-40}$ esu² cm². The sign of the net CD predicted for (1*S*,5*S*)-**1** is the same as that observed for (+)-**1**. The DFT CD calculations thus lead to the conclusion that the AC of **1** is (1*S*,5*S*)-(+)/(1*R*,5*R*)-(-), in agreement with all previous assignments.

(c) Optical rotation: Hoffmann and Wiartalla¹² reported $[\alpha]_{\text{D}} = +212$ (c 1.3, dioxane) for enantiomerically pure (+)-**1**. Berg and Butkus⁹ reported $[\alpha]_{\text{D}}^{25} = -101$ (c 0.1, dioxane) for (-)-**1** of 50% ee, corresponding to a value of -202 for optically pure **1**. Malinauskiene et al.¹⁵ reported $[\alpha]_{\text{D}} = -197$ (c 0.2–0.3, dioxane) for enantiomerically pure (-)-**1**. Butkus et al.^{11,14} reported $[\alpha]_{\text{D}}^{18} = +204.0$ (c 0.05, dioxane) for (+)-**1** of 93% ee, corresponding to a value of +219 for optically pure **1**. In this work,

we have remeasured the specific rotation of (+)-**1** of ee >99% at several wavelengths and in three solvents, dioxane, methanol, and acetone, with the results given in Table 1.

Specific rotations of the conformations of (1*S*,5*S*)-**1** have been predicted at the B3LYP/6-31G* geometries, using B3LYP and the aug-cc-pVDZ basis set. The results are given in Table 1, together with population-weighted average specific rotations. At the sodium D line, the CC and CB conformations are both predicted to exhibit positive rotations, leading to a positive average rotation and the conclusion that the AC of **1** is (1*S*,5*S*)-(+)/(1*R*,5*R*)-(-), consistent with prior assignments and with the AC arrived at above from the DFT analysis of the CD spectrum. Predicted $[\alpha]$ values of **1** increase in magnitude with decreasing wavelength (up to 365 nm), as do the experimental $[\alpha]$ values.

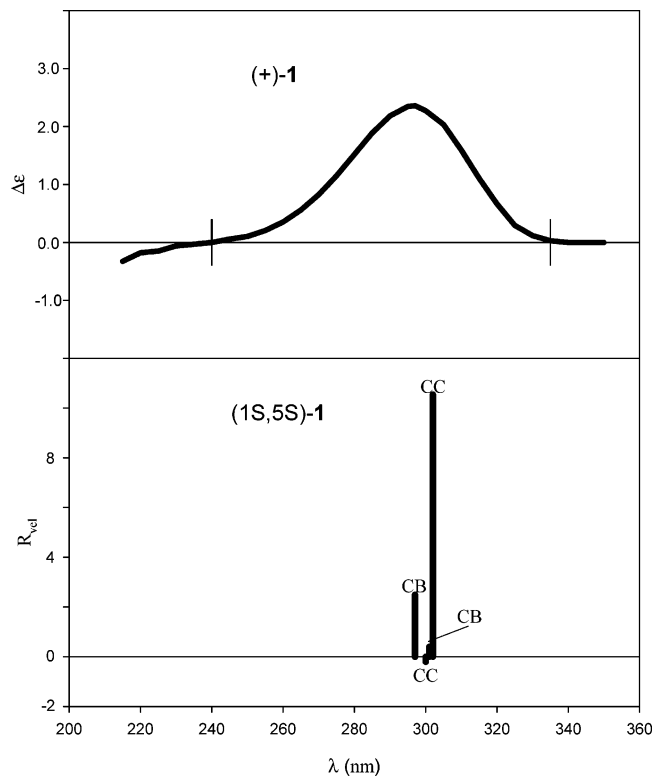


FIGURE 1. Calculated and experimental CD of **1**. The experimental CD is for (+)-**1** of >99% ee in 95% ethanol. Vertical lines indicate the integration range used in obtaining experimental rotational strengths. The calculated rotational strengths, R_{vel} , are for (1*S*,5*S*)-**1**.

Bicyclo[3.3.1]nonane-2,7-dione (2). (a) **Conformational analysis:** MMFF94 calculations by Butkus et al.¹¹ found two conformations of **2**, chair-chair (CC) and chair-boat (CB), the latter being higher in energy. In this work, we have carried out conformational analysis of **2** using the CFF95, MMFF94, AM1, PM3, HF/6-31G**, and B3LYP/6-31G* methods. Our results are given in Table 2. All methods predict that the CC conformation is lowest in energy. CFF95, AM1, and PM3 methods predict that both chair-boat (CB) and boat-chair (BC) conformations are stable; the CFF95 energies are very different, while the AM1 and PM3 energies are similar. In contrast, the MMFF94, HF/6-31G**, and B3LYP/6-31G* methods predict that the CB and BC conformations are stable and unstable, respectively. The most reliable method, B3LYP/6-31G*, predicts that the CB conformation is 3.26 kcal/mol higher in energy than the CC conformation. All methods predict only one boat-boat (BB) conformation. With the exception of the CFF95 method, the BB conformation is the highest in energy. With the B3LYP/6-31G* method, the BB conformation is 6.16 kcal/mol higher in energy than the CC conformation. At the B3LYP/6-31G* level, relative free energies (ΔG) have been calculated in addition to relative energies (ΔE), with the results given in Table 2. ΔE and ΔG values are very similar. Percentage populations have been calculated based on ΔE and ΔG values, using Boltzmann statistics and $T = 298$ K, with the results given in Table 2. At room temperature, we predict that the CC conformation is >99% of the equilibrium mixture of CC, CB, and BB

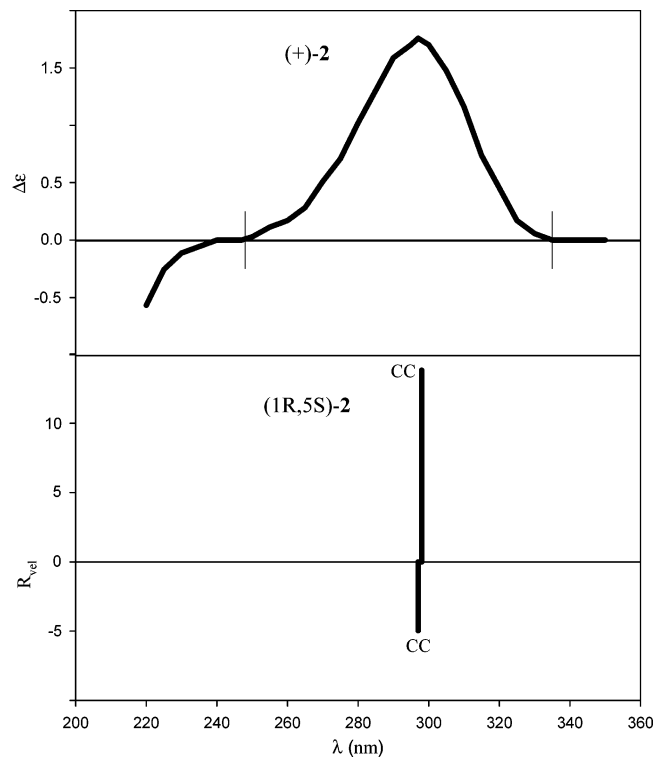


FIGURE 2. Calculated and experimental CD of **2**. The experimental CD is for (+)-**2** of 100% ee in 95% ethanol. Vertical lines indicate the integration range used in obtaining experimental rotational strengths. The calculated rotational strengths, R_{vel} , are for (1*R*,5*S*)-**2**.

conformers, a conclusion consistent with the earlier work of Butkus et al.¹¹

(b) **Electronic CD:** Butkus et al.¹¹ reported the experimental CD of **2**. Positive CD, attributable to the $n \rightarrow \pi^*$ transitions of the C=O groups of **2**, was observed for (+)-**2** at ~ 295 nm. Application of the Octant Rule did not unambiguously define the AC of **2**, although the AC (1*R*,5*S*)-(+)/(1*S*,5*R*)-(-) was concluded to be more likely. This AC was confirmed by synthesis of **2**, starting from **1**.

In this work, we have remeasured the UV CD of **2**, using a sample of (+)-**2** of much higher ee (100%) than that used previously (55%). The spectrum is shown in Figure 2. Integration of the CD (over the range 248–335 nm) yields an experimental value for the net rotational strength of the $n \rightarrow \pi^*$ transitions of $+5.0 \times 10^{-40}$ esu² cm².

Excitation energies, oscillator strengths, and rotational strengths predicted for the conformations of (1*R*,5*S*)-**2** with B3LYP and aug-cc-pVDZ are given in Table 2. For each conformation, two $n \rightarrow \pi^*$ transitions are predicted within the range 295–305 nm, well-separated from the next-highest excitations. The CD spectrum of the equilibrium mixture of conformers is plotted in Figure 2. Due to the >99% population of the CC conformer, only this conformer contributes significantly. The two $n \rightarrow \pi^*$ transitions of the CC conformer are at 298 and 297 nm. Their rotational strengths are of opposite sign, the positive R value of the lower transition being much larger in magnitude than the negative R value of the higher transition. The population-weighted net R value of the

TABLE 2. 2,7-Dione, 2: Conformational Energies, Specific Rotations, and Circular Dichroism

Conformations ^a									
	CFF95	MMFF94	AM1	PM3					
CC	0	0	0	0					
CB ^b	3.88	3.20 ^c	1.50	1.95					
BC ^b	8.86		1.87	2.10					
BB	8.56	8.62	3.52	4.47					
B3LYP/6-31G*									
	HF/6-31G**	ΔE	ΔG	$P(\Delta E)^d$	$P(\Delta G)^d$				
CC	0	0	0	99.59	99.41				
CB ^b	3.56	3.26	3.04	0.41	0.59				
BC ^b									
BB	6.84	6.16	6.02	0.00	0.00				
Specific Rotation									
calcd ^e [α]									
λ	CC	CB	BB	av(ΔE) ^g	av(ΔG) ^g	exptl ^f [α]			
D	184	-63	-308	183	182	145			
578						154			
546	226	-76	-371	225	224	182			
436						355			
365	1038	-236	-1277	1033	1031	721			
Circular Dichroism									
calcd ^e for CC					exptl ^h				
E (eV)	λ (nm)	f^j	R_{vel}^i	R_{length}^i	λ (nm)	R^i			
4.157	298	0.0002	13.86	14.10	297	5.0			
4.170	297	0.0002	-4.98	-4.92					
5.022	247	0.0016	-5.32	-5.53					
5.289	234	0.0003	0.22	0.19					
calcd ^e for CB					calcd ^e for BB				
E (eV)	λ (nm)	f^j	R_{vel}^i	R_{length}^i	E (eV)	λ (nm)	f^j	R_{vel}^i	R_{length}^i
4.061	305	0.0001	-3.29	-3.06	4.121	301	0.0001	-6.96	-6.27
4.116	301	0.0001	4.40	4.33	4.188	296	0.0001	1.98	1.42
5.054	245	0.0020	3.21	3.12	4.952	250	0.0021	5.05	4.64
5.102	243	0.0014	-12.12	-12.64	5.366	231	0.0042	1.82	1.56

^a Relative energies in kcal/mol. For B3LYP/6-31G*, relative free energies in kcal/mol are also given. ^b C(7)=O in chair, C(2)=O in boat in CB; C(7)=O in boat, C(2)=O in chair in BC. ^c 1.6 kcal/mol in ref 11. ^d Percentage populations obtained from B3LYP/6-31G* ΔE and ΔG values, using Boltzmann statistics and $T = 298$ K. ^e B3LYP/avg-cc-pVDZ at the B3LYP/6-31G* geometry of each conformation. AC is 1*R*,5*S*. ^f For (+)-**2**: solvent is 95% EtOH (c 0.08); ee is 100% (chiral chromatography). ^g av(ΔE) and av(ΔG) [α] values are conformational averages based on B3LYP/6-31G* ΔE and ΔG values, respectively. ^h For (+)-**2**: solvent is 95% EtOH; ee is 100% ee (chiral chromatography). ⁱ R values in 10^{-40} esu² cm². ^j Oscillator strengths.

$n \rightarrow \pi^*$ transitions of the equilibrium mixture of CC, CB, and BB conformers is $+8.8 \times 10^{-40}$ esu² cm². The sign of the net CD predicted for (1*R*,5*S*)-**2** is the same as that observed for (+)-**2**. The DFT CD calculations thus lead to the conclusion that the AC of **2** is (1*R*,5*S*)-(+)/(1*S*,5*R*)-(-), in agreement with the AC arrived at by Butkus et al., both from the UV CD and on the basis of synthesis from **1**.¹¹

(c) Optical rotation: Butkus et al.¹¹ reported [α]₅₄₆¹⁶ = +117.7 (c 0.045, CHCl₃) for (+)-**2** of 55% ee, corresponding to a value of 214 for optically pure **2**. In this work, we have remeasured the specific rotation of (+)-**2** of 100% ee in 95% EtOH at several wavelengths, with the results given in Table 2.

Specific rotations of the conformations of (1*R*,5*S*)-**2** have been predicted using B3LYP and aug-cc-pVDZ with the results given in Table 2, together with population-weighted average specific rotations. Agreement between rotations predicted for (1*R*,5*S*)-**2** and experimental rotations for (+)-**2** is good. At the sodium D line, predicted

and experimental rotations are 182 and 145, respectively; at 546 nm the values are 224 and 182. Since the experimental rotation at 546 nm in CHCl₃, 214, is closer to the predicted value than the rotation in 95% EtOH, the differences between predicted and experimental values may be in part due to solvent effects. The good agreement of predicted and experimental specific rotations leads to the conclusion that the AC of **2** is (1*R*,5*S*)-(+)/(1*S*,5*R*)-(-), in agreement with the earlier work of Butkus et al.¹¹ and the DFT analysis of the CD above.

Bicyclo [3.3.1]nonane-2,9-dione (3). **(a) Conformational analysis:** MM2 calculations by Berg and Butkus^{9,10} found two conformations of **3**, chair-chair (CC) and chair-boat (CB), the latter (surprisingly) being lower in energy by 0.44 kcal/mol than the former. Alkauskas et al.²⁸ carried out a more thorough investigation of the conformations of **3** using the HF/6-31G and HF/6-31G** methods and identified CC, CB, boat-chair (BC), and two boat-boat (BB) conformations. Their results are given in Table 3. Consistent with the prior MM2 calculations, the

TABLE 3. 2,9-Dione, **3**: Conformational Energies, Specific Rotations, and Circular Dichroism

Conformations ^a																		
		MM2 ^b			CFF95			MMFF94			AM1		PM3					
CC		0.44			0			0			0.59		0					
CB ^c		0			0.75			0.75			0		1.25					
BC ^c					4.80			4.30			1.38		2.47					
BBa					7.05			7.77										
BB											2.88		4.63					
BBb					7.14			8.54										
		HF/6-31G ^d			HF/6-31G ^{**}			B3LYP/6-31G [*]										
		ΔH			ΔE			ΔE			ΔG		$P(\Delta E)^e$		$P(\Delta G)^e$			
CC		0.69			0.53			0.60			0.11		0.07		44.97		46.82	
CB		0			0			0			0		54.47		52.61			
BC		3.78			3.65			3.68			2.75		2.74		0.53		0.52	
BBa		4.81			4.99			4.88			4.37		4.17		0.03		0.05	
BB																		
BBb		6.79			6.67			6.58			5.95		5.68		0.00		0.00	
Specific Rotation																		
calcd ^f [α]																		
λ (nm)	CC		CB		BC		BBa		BBb		av(ΔE)		av(ΔG)		exptl [α]			
D	-6		255		-51		243		149		136		131		-108, ^g +97/-97 ^h			
546	-5		312		-62		292		186		167		162					
365	93		1213		-310		818		782		701		680					
Circular Dichroism																		
calcd ^f for CC					calcd ^f for CB					expt ⁱ								
E (eV)	λ (nm)	f^k	R_{vel}^j	R_{length}^j	E (eV)	λ (nm)	f^k	R_{vel}^j	R_{length}^j	λ (nm)	R^l							
4.003	310	0.0025	-0.86	-0.84	4.139	300	0.0001	-2.76	-2.35	281,308	+1.5							
4.231	293	0.0001	2.56	2.68	4.205	295	0.0001	7.89	7.67									
5.056	245	0.0039	1.30	1.42	4.885	254	0.0004	1.41	1.61									
5.623	220	0.0488	7.85	7.71	5.429	228	0.0263	21.71	21.96									
calcd ^f for BC					calcd ^f for BBa					calcd ^f for BBb								
E (eV)	λ (nm)	f^k	R_{vel}^j	R_{length}^j	E	λ	f^k	R_{vel}^j	R_{length}^j	E (eV)	λ (nm)	f^k	R_{vel}^j	R_{length}^j				
4.001	310	0.0035	-5.95	-6.82	4.165	298	0.0000	-1.91	-2.08	4.057	306	0.0014	-11.01	-11.33				
4.237	293	0.0005	8.79	8.80	4.235	293	0.0000	-2.07	-2.09	4.280	290	0.0008	25.77	26.70				
5.157	240	0.0017	-0.10	0.09	4.860	255	0.0004	7.25	7.64	5.095	243	0.0006	-0.53	-0.56				
5.672	219	0.0478	-8.53	-8.91	5.423	229	0.0243	28.30	28.78	5.513	225	0.0408	-8.21	-8.45				

^a Relative energies in kcal/mol. For B3LYP/6-31G* relative free energies in kcal/mol are also given. ^b References 9 and 10. ^c C(2)=O in boat in CB; C(2)=O in chair in BC. ^d Reference 28. ^e Percentage populations obtained from B3LYP/6-31G* ΔE and ΔG values, using Boltzmann statistics and $T = 298$ K. ^f B3LYP/aug-cc-pVDZ at the B3LYP/6-31G* geometry of each conformation. AC is 1S,5R. ^g In 95% EtOH (c 0.1) for (-)-**3** of ee 50% [ref 9]; normalized to 100% ee. ^h In CHCl₃ (c 0.005) for (+)-**3**/(-)-**3** of ee 81/70% [ref 18]; normalized to 100% ee. ⁱ For (+)-**3**: in 95% EtOH; ee 80%. R value is normalized to 100% ee. ^j R values in 10⁻⁴⁰ esu² cm². ^k Oscillator strengths.

CB conformation was predicted to be lower in energy than the CC conformation. In this work, we have further studied the conformations of **3** using the CFF95, MMFF94, AM1, PM3, HF/6-31G**, and B3LYP/6-31G* methods, with the results given in Table 3. As with MM2 and HF/6-31G**, AM1 and B3LYP/6-31G* predict CB to be the lowest energy conformation. In contrast, CFF95, MMFF94, and PM3 predict that CC is lower in energy than CB. The CFF95, MMFF94, HF/6-31G**, and B3LYP/6-31G* methods all predict two stable boat-boat (BB) conformations, lying at substantially higher energies than the CC, CB, and BC conformations. In contrast, the AM1 and PM3 methods predict only one stable BB conformation. At the B3LYP/6-31G* level, relative free energies (ΔG) have been calculated in addition to relative energies (ΔE), with the results given in Table 3. ΔE and ΔG values are very similar. Percentage populations based on ΔE and ΔG values at $T = 298$ K are given in Table 3. At room temperature, we predict that the CC and CB conformers

are comparably populated, and that together they constitute >99% of the equilibrium mixture of CC, CB, BC, and BB conformers, consistent with the earlier work of Berg and Butkus.^{9,10}

(b) Electronic CD: Berg and Butkus⁹ reported the experimental UV CD of **3**. Negative CD, attributable to the $n \rightarrow \pi^*$ transitions of the C=O groups of **3**, was observed at ~280 nm for (-)-**3**. Assuming the CB conformation to be predominant, application of the Octant Rule led to the AC (1S,5R)-(-). Subsequently, Berg and Butkus¹⁰ predicted the CD of **3** using a methodology of Tinoco and Schellman and assuming a population distribution of 75% CB and 25% CC. Negative CD was predicted for 1R,5S-**3** at ~280 and ~210 nm, consistent with the experimental CD of (-)-**3**, leading to a reversal of the AC to (1R,5S)-(-).

In this work, we have remeasured the CD of **3** using a sample of (+)-**3** of higher ee (80%) than used previously (50%).⁹ The spectrum is shown in Figure 3. Consistent

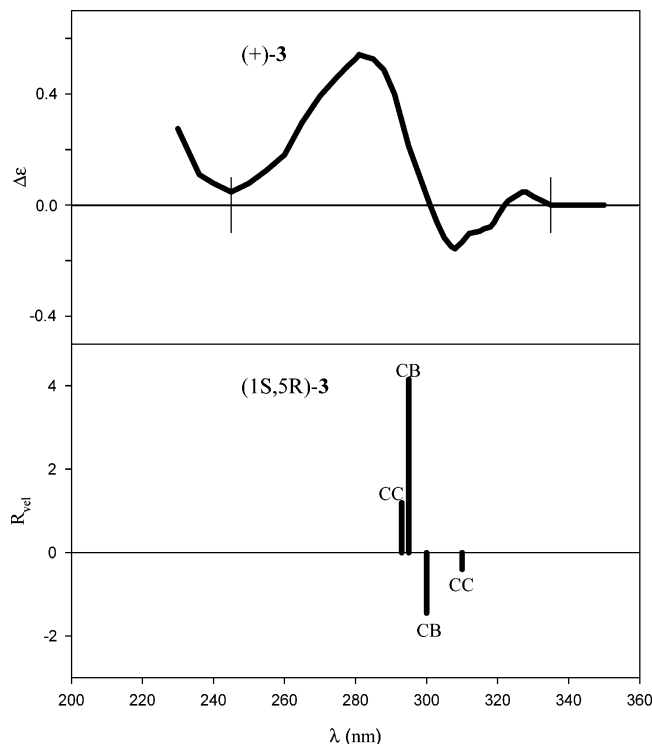


FIGURE 3. Calculated and experimental CD of **3**. The experimental CD is for (+)-**3** of ee 80% in 95% ethanol, normalized to 100% ee. Vertical lines indicate the integration range in obtaining experimental rotational strengths. The calculated rotational strengths are for (1*S*,5*R*)-**3**.

with the earlier work, positive CD is observed at ~280 nm for (+)-**3**. However, in addition, negative CD is observed at >300 nm and positive CD at >320 nm.

Excitation energies, oscillator strengths, and rotational strengths predicted for the conformations of (1*S*,5*R*)-**3** using B3LYP and aug-cc-pVDZ are given in Table 3. For each conformation two $n \rightarrow \pi^*$ transitions are predicted within the range 290–310 nm, well-separated from the next-highest excitations. The CD spectrum of the equilibrium mixture of conformers is plotted in Figure 3. Due to the >99% population of the CC and CB conformers, only these two conformers contribute significantly. Two $n \rightarrow \pi^*$ transitions are predicted for the CB conformation at 300 and 295 nm, with negative and positive rotational strengths, respectively. For the CC conformation two $n \rightarrow \pi^*$ transitions are predicted at 310 and 293 nm with negative and positive rotational strengths. As a result, the predicted CD of the equilibrium mixture exhibits negative CD at longer wavelengths and positive CD at shorter wavelengths. With the exception of the weak CD at wavelengths >320 nm, the predicted CD of (1*S*,5*R*)-**3** is in good agreement qualitatively with the experimental CD of (+)-**3**. The 310- and 300-nm transitions of CC and CB are assigned to the longer wavelength negative CD; the 295- and 293-nm transitions of CB and CC are assigned to the shorter wavelength positive CD. Quantitatively, the population-weighted net R value of the $n \rightarrow \pi^*$ transitions of the equilibrium mixture of CC, CB, BC, and BB conformers is $+3.5 \times 10^{-40}$ esu² cm². Integration of the CD (over the range 245–335 nm) yields an experimental value for the net rotational strength of the $n \rightarrow \pi^*$ transitions of $+1.5 \times 10^{-40}$ esu² cm². The DFT

calculations thus lead to the conclusion that the AC of **3** is (1*S*,5*R*)-(+)/(1*R*,5*S*)-(-), as arrived at in the later analysis of Berg and Butkus¹⁰ and, subsequently, via asymmetric synthesis of **3**.¹⁸

(c) Optical rotation: Berg and Butkus⁹ reported $[\alpha]_D^{25} = -54$ (c 0.1, 95% EtOH) for (-)-**3** of 50% ee, corresponding to a value of -108 for optically pure **3**. Butkus and Stoncius¹⁸ reported $[\alpha]_D^{20}$ values of -67.8 and +78.5 (c 0.005, CHCl₃) for (-)- and (+)-**3** of 70% and 81% ee, respectively, corresponding to -96.9 and +96.9 for optically pure **3**.

Specific rotations of the conformations of (1*S*,5*R*)-**3** have been predicted using B3LYP and aug-cc-pVDZ, with the results given in Table 3, together with population-weighted average specific rotations. At the sodium D line, the CC and CB conformations are predicted to exhibit small negative and large positive rotations, respectively, leading to a net positive rotation and the conclusion that the AC of **3** is (1*S*,5*R*)-(+)/(1*R*,5*S*)-(-). This AC is that deduced by Berg and Butkus¹⁰ via Tinoco–Schellman calculations, by Butkus and Stoncius¹⁸ via asymmetric synthesis of **3**, and, in this work, via the DFT analysis of the CD above.

exo-7-Methyl-bicyclo[3.3.1]nonane-2,9-dione (**4**).

(a) Conformational analysis: The 7-Me substitution of **3** to give **4** is a minor perturbation to the conformational energetics of **3**. In view of the results obtained for **3** (Table 3) we have limited conformational analysis of **4** to the B3LYP/6-31G* method and to the CC and CB conformations. As with **3**, the CB conformer is found to be lower in energy than CC. ΔE and ΔG values are very similar to those for **3**. Accordingly, at room temperature we predict that the CC and CB conformers are comparably populated.

(b) Electronic CD: The CD spectrum of a sample of (-)-**4** of ee 83% is shown in Figure 4. The spectrum mirror images the CD spectrum of (+)-**3** to a very good approximation, leading immediately to the expectation that (+)-**3** and (+)-**4** possess identical ACs at C1 and C5.

Excitation energies, oscillator strengths, and rotational strengths predicted for the CC and CB conformations of (1*R*,5*R*,7*R*)-**4** using B3LYP and aug-cc-pVDZ are given in Table 4. The results are qualitatively identical with those for **3**. For each conformer two $n \rightarrow \pi^*$ transitions are predicted within the range 290–310 nm, well-separated from the next-highest excitations. The CD spectrum of the equilibrium mixture of conformers is plotted in Figure 4. With the exception of the weak positive CD at wavelengths >320 nm, the predicted CD of (1*R*,5*R*,7*R*)-**4** is in excellent agreement qualitatively with the experimental CD of (-)-**4**. Quantitatively, the population-weighted net R value of the $n \rightarrow \pi^*$ transitions of the equilibrium mixture of CC and CB conformers is -3.8×10^{-40} esu² cm². Integration of the CD (over the range 247–335 nm) yields an experimental value for the net rotational strength of the $n \rightarrow \pi^*$ transitions of -1.6×10^{-40} esu² cm². The DFT calculations thus lead to the conclusion that the AC of **3** is (1*S*,5*S*,7*S*)-(+)/(1*R*,5*R*,7*R*)-(-), as concluded previously from the asymmetric synthesis of **4**.¹⁸

(c) Optical rotation: Butkus and Stoncius¹⁸ reported $[\alpha]_D^{20}$ values of +20.0 and -19.1 (c ~0.005, CHCl₃) for

TABLE 4. *exo*-7-Me-2,9-Dione, **4**: Conformational Energies, Specific Rotations, and Circular Dichroism

Conformations ^a											
B3LYP/6-31G*											
		ΔE	ΔG	$P(\Delta E)^b$	$P(\Delta G)^b$						
CC ^c		0.15	0.12	43.52	45.12						
CB ^c		0	0	56.48	54.88						
Specific Rotation											
calcd ^d [α]											
λ (nm)	CC	CB	Av(ΔE)	Av(ΔG)	exptl [α]						
D	14	-243	-131	-127	+23.0/-23.0 ^e						
546	15	-297	-161	-156							
365	20	-1151	-642	-623							
Circular Dichroism											
calcd ^d for CB					calcd ^d for CC					exptl ^g	
E (eV)	λ (nm)	f^h	R_{vel}^f	R_{length}^f	E (eV)	λ (nm)	f^h	R_{vel}^f	R_{length}^f	λ (nm)	R^f
3.997	310	0.0025	2.91	2.84	4.133	300	0.0002	4.70	4.47	281, 308	-1.6
4.226	293	0.0001	-4.09	-4.29	4.210	295	0.0001	-10.68	-10.65		
5.053	245	0.0037	-1.18	-1.29	4.899	253	0.0004	-1.36	-1.54		
5.611	221	0.0461	-6.79	-6.72	5.412	229	0.0255	-20.31	-20.49		

^a Relative energies and free energies in kcal/mol. ^b Percentage populations obtained from B3LYP/6-31G* ΔE and ΔG values, using Boltzmann statistics. ^c C(2)=O in boat in CB; C(2)=O in chair in BC. ^d B3LYP/aug-cc-pVDZ at the B3LYP/6-31G* geometry of each conformation. The AC is 1*R*,5*R*,7*R*. ^e $[\alpha]_D^{20}$ for (+)-**4**/(-)-**4**, measured in CHCl₃ (*c* 0.0055/0.0048) on samples of 87%/83% ee [ref 18]; normalized to 100% ee. ^f R values in 10⁻⁴⁰ esu² cm². ^g For (-)-**4**: solvent is 95% EtOH; ee 83%; R value is normalized to 100% ee. ^h Oscillator strengths.

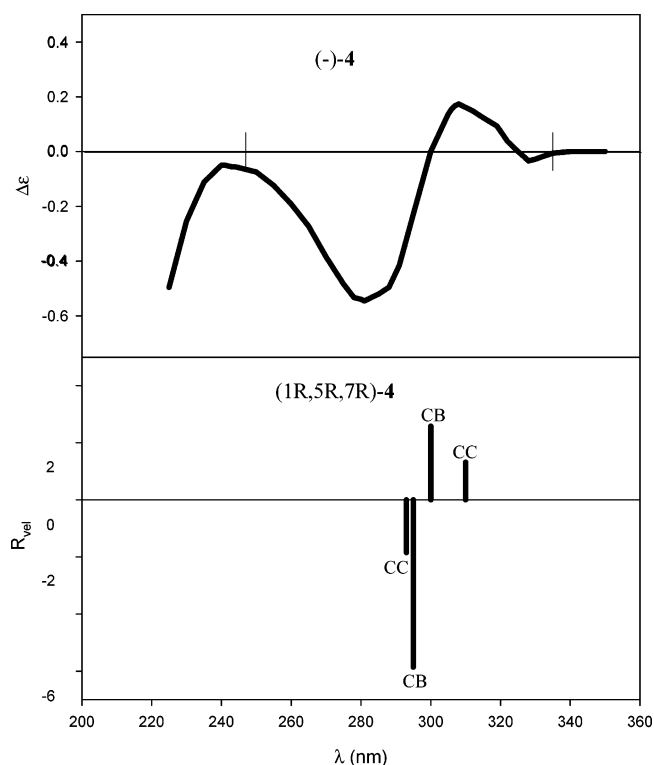


FIGURE 4. Calculated and experimental CD of **4**. The experimental CD is for (-)-**4** of ee 83% in 95% ethanol, normalized to 100% ee. Vertical lines indicate the integration range used in obtaining experimental rotational strengths. The calculated rotational strengths are for (1*R*,5*R*,7*R*)-**4**.

(+)- and (-)-**4** of 87% and 83% ee, respectively, corresponding to +23.0 and -23.0 for optically pure **4**.

Specific rotations of the CC and CB conformations of (1*R*,5*R*,7*R*)-**4** have been predicted using B3LYP and aug-

cc-pVDZ, with the results given in Table 4, together with the population-weighted average specific rotations. Predicted rotations are very close to those predicted for (1*R*,5*S*)-**3** (Table 3), a result inconsistent with the reported reduction in experimental $[\alpha]_D$ by a factor of ~4. A possible explanation may be that this compound is relatively unstable and undergoes ring-reopening reaction, even at room temperature. New measurements of the specific rotation of **4** are desirable to determine the source of this discrepancy.

Discussion

The AC of **1** is based on stereochemically well-defined synthesis and on analyses of the $n \rightarrow \pi^*$ C=O CD using the Octant Rule and the Tinoco–Schellman methodology, which all yield the same AC. Our TDDFT calculations of the $n \rightarrow \pi^*$ C=O CD of **1** yield CD of the same sign as predicted by the Octant Rule and the Tinoco–Schellman calculations and, hence, the same AC. Our TDDFT calculations of the specific rotation of **1** lead independently to the same AC.

The AC of **2** is based on stereochemically well-defined synthesis (from **1**) and on analysis of the $n \rightarrow \pi^*$ C=O CD using the Octant Rule, although the Octant Rule analysis was not unambiguous. Our TDDFT calculations of the $n \rightarrow \pi^*$ C=O CD of **2** yield the same AC as obtained earlier. Our TDDFT calculations of the specific rotation of **2** lead independently to the same AC.

The AC of **3** was originally obtained by analysis of the $n \rightarrow \pi^*$ C=O CD using the Octant Rule. Subsequently, calculation of the CD with the Tinoco–Schellman methodology led to a reversal of the AC. The revised AC was later supported by a mechanistic analysis of the synthesis of **3** via asymmetric cyclization. Our TDDFT calculations of the $n \rightarrow \pi^*$ C=O CD of **3** yield the same AC as obtained

from the Tinoco–Schellman calculations, confirming the incorrectness of the Octant Rule analysis for this molecule. Our TDDFT calculations of the specific rotation of **3** lead independently to the same AC as the TDDFT CD calculations.

The AC of **4** was obtained by means of mechanistic analysis of the synthesis of **4** via asymmetric cyclization. Our TDDFT calculations of the $n \rightarrow \pi^*$ C=O CD and of the specific rotation of **4** both lead to the same AC.

Thus, for the set of diketones **1–4** our TDDFT calculations of the $n \rightarrow \pi^*$ C=O CD and of the specific rotations are consistent with, and add support to, the previously assigned ACs. In particular, (1) the reliability of the Octant Rule analyses for **1** and **2** and the unreliability of the analysis for **3** are confirmed and (2) the mechanistic analysis of the 2-(methoxymethyl)pyrrolidine enamine asymmetric syntheses of **3** and **4** is supported.

Our results for **1–4** provide further evidence regarding the accuracy of TDDFT calculations of OR and CD. The comparison of theory and experiment is simplest in the case of **2**, where only one conformation is populated. The predicted specific rotations of **2** at the sodium D line and at 546 nm are in good agreement with the experimental values. The deviations of calculated rotations from experiment are within the range found in previous studies of conformationally rigid molecules^{2a} and are most likely attributable to the imperfection of the B3LYP functional, vibrational effects, and/or solvent effects. That solvent effects are not negligible is clearly shown by the significant difference in $[\alpha]_{546}$ in 95% ethanol and CHCl₃. The predicted sum of the C=O $n \rightarrow \pi^*$ R_{vel} values is also in good agreement with the experimentally derived rotational strength. To date, there has been no thorough study of the quantitative accuracy of TDDFT rotational strengths of $n \rightarrow \pi^*$ C=O transitions. It is likely that the deviation of calculated rotational strengths from experiment is attributable principally to vibronic effects and/or to solvent effects.

In the case of molecules **1**, **3**, and **4**, calculated CD rotational strengths and specific rotations are conformationally averaged. Errors in the conformational populations used will lead to additional errors in predicted rotational strengths and specific rotations.^{4b} In this work, conformational populations are obtained from relative ΔG values, calculated at the B3LYP/6-31G* level. Some uncertainty is associated with the B3LYP/6-31G* method; in addition, our ΔG calculations do not include solvent effects, which can significantly affect relative free energies. Thus, predicted conformationally averaged rotational strengths and specific rotations for **1** are greater than experimental values. Since the CB conformation exhibits smaller rotational strengths and specific rotations than the CC conformation, decreasing the free energy difference of CB and CC would lead to smaller rotational strengths and specific rotations and, as a result, better agreement with experiment. Likewise, for **3**, reducing and increasing the populations of the CB and CC conformations respectively would bring predicted rotational strengths and specific rotations into better agreement with experiment. It is likely that for **1** and **3** the uncertainties in conformational free energy differences and populations are the dominant cause of differences between theory and experiment. In the case of **4**, as discussed above, experimental error may be dominant.

TABLE 5. OR and CD Additivity^a

	CC		CB	
	$[\alpha]_{\text{D}}$	R^e	$[\alpha]_{\text{D}}$	R^e
2,6-dione, 1 ^b				
2-one + 6-one	+346	+12.5	+14	+4.4
2,6-dione	+334	+14.3	+70	+10.6
2,7-dione, 2 ^c				
2-one + 7-one	+172	+7.1		
2,7-dione	+184	+8.9		
2,9-dione, 3 ^d				
2-one + 9-one	-156	-5.1	154	2.3
2,9-dione	-6	1.7	255	5.1

^a All calculations used B3LYP and aug-cc-pVDZ. The geometries of the monoketones *x*-one and *y*-one, corresponding to the *x,y*-dione, were obtained by replacing the O atoms at the *y* and *x* positions with two H atoms respectively and optimizing their positions at the B3LYP/6-31G* level. Note that, with this methodology, the 7-one and 9-one monoketones are not perfectly achiral; their $[\alpha]_{\text{D}}$ and R values are small, however. ^b (1*S*,5*S*)-**1**. ^c (1*R*,5*S*)-**2**. ^d (1*S*,5*R*)-**3**. ^e Sum of R_{vel} values for the $n \rightarrow \pi^*$ C=O transitions; in 10^{-40} esu² cm².

Since conformational analysis of organic molecules such as **1–4** is often carried out with molecular mechanics and semiempirical methods, we have compared the results obtained for **1–4** using the CFF95 and MMFF94 molecular mechanics methods and the AM1 and PM3 semiempirical methods to those obtained using DFT. Substantial differences from the DFT results are found for all of these methods in one or more molecules; in addition, neither the two molecular mechanics methods nor the two semiempirical methods are very consistent in their predictions. The use of CFF95, MMFF94, AM1, or PM3 structures and energies would thus lead to substantially different predicted CD rotational strengths and specific rotations. For conformationally flexible molecules, the use of the more reliable DFT method in carrying out conformational analysis is of importance.

Our work extends the scope of the application of chiroptical spectroscopic methods to the characterization of **1–4** by including OR in addition to CD. OR and CD are related phenomena. However, while the near-UV CD spectrum reflects the rotational strengths of the low-energy electronic excitations, the OR in the transparent spectral region to lower energy reflects the rotational strengths of **all** electronic excitations. The use of both phenomena in stereochemical analysis is thus not redundant. For example, it is possible for the $n \rightarrow \pi^*$ C=O CD to be small and for $[\alpha]_{\text{D}}$ to be large, or vice versa. Only if the specific rotation is dominated by the contribution of the $n \rightarrow \pi^*$ C=O CD are the two phenomena redundant. The study of both OR and CD simultaneously, using consistent theoretical methods, thus yields a more definitive analysis than does the study of either OR and CD alone. In particular, when used to determine AC, the reliability of the AC obtained is more clearly defined when both OR and CD are used. If OR and CD yield the same AC it is more definitive than if obtained from only the OR or the CD alone. Conversely, if the OR and CD yield opposite ACs, the AC must be regarded as indeterminate.

The chirality of the diones **1–4** arises from C=O group substitutions on an achiral bicyclo[3.3.1]nonane substrate. If the two C=O groups are noninteracting, the

chiroptical properties of a dione will be the sum of those of the two corresponding monoketones. If there is “trans-annular” interaction, nonadditivity will result.²⁹ Thus, the magnitude of the nonadditivity of chiroptical properties can be used as a gauge of the interaction of the two C=O groups. In Table 5, we examine the additivity of the specific rotations, $[\alpha]_D$, and the net $n \rightarrow \pi^*$ C=O rotational strengths of the important conformations of **1**, **2**, and **3**. For the CC conformations of **1** and **2**, nonadditivity is small for both specific rotations and rotational strengths. However, substantial nonadditivity is found for the CB conformation of **1** and for both CC and BC conformations of **3** for both specific rotations and rotational strengths. The greater nonadditivities in **3** probably result from the greater proximity of the two C=O groups.

(29) Lightner, D. A.; Gurst, J. E. *Organic Conformational Analysis and Stereochemistry from Circular Dichroism Spectroscopy*; Wiley: New York, 2000; Chapter 10, pp 305–335.

Conclusion

We have illustrated the use of concerted TDDFT calculations of OR and CD in determining the absolute configurations of chiral molecules. While the present work is limited to bicyclo[3.3.1]nonane diones, the methodology is general and should be widely applicable.

Acknowledgment. We acknowledge financial support of this research by the Lithuanian science and studies foundation (grant C-02/2003 to E.B.) and by the U.S. National Science Foundation (grant CHE-0209957 to P.J.S.). We are also grateful to the USC Center for High Performance Computing for computer time.

Supporting Information Available: Text files containing B3LYP/6-31G*-optimized Cartesian coordinate geometries of molecules **1–4**. This material is available free of charge via the Internet at <http://pubs.acs.org>.

JO0357061